



# Laser Scanning Systems and Techniques in Rockfall Source Identification and Risk Assessment: A Critical Review

Ali Mutar Fanos<sup>1</sup> · Biswajeet Pradhan<sup>2</sup> 

Received: 27 December 2017 / Accepted: 2 April 2018  
© Springer International Publishing AG, part of Springer Nature 2018

## Abstract

Rockfall poses risk to people, their properties and to transportation ways in mountainous and hilly regions. This catastrophe shows various characteristics such as vast distribution, sudden occurrence, variable magnitude, strong fatalness and randomness. Therefore, prediction of rockfall phenomenon both spatially and temporally is a challenging task. Digital Terrain model (DTM) is one of the most significant elements in rockfall source identification and risk assessment. Light detection and ranging (LiDAR) is the most advanced effective technique to derive high-resolution and accurate DTM. This paper presents a critical overview of rockfall phenomenon (definition, triggering factors, motion modes and modeling) and LiDAR technique in terms of data pre-processing, DTM generation and the factors that can be obtained from this technique for rockfall source identification and risk assessment. It also reviews the existing methods that are utilized for the evaluation of the rockfall trajectories and their characteristics (frequency, velocity, bouncing height and kinetic energy), probability, susceptibility, hazard and risk. Detail consideration is given on quantitative methodologies in addition to the qualitative ones. Various methods are demonstrated with respect to their application scales (local and regional). Additionally, attention is given to the latest improvement, particularly including the consideration of the intensity of the phenomena and the magnitude of the events at chosen sites.

**Keywords** Rockfall · LiDAR · Risk · Hazard · Remote sensing · GIS

## 1 Introduction

Rockfall is a common and widespread phenomenon that can influence entire villages, extended stretches of transportation routes, isolated accommodations, and other anthropic goods, in which these elements at risk are situated near or on the bases of steep rock slope. Because of its unpredictability and vast velocity, rockfall event can result in casualties, even with very small volume (less than 1 m<sup>3</sup>) of the mobilized mass. Rockfall risk is normally assessed via employing two-dimensional (2D) or three-dimensional (3D) simulation models, with the goal of estimating runout distances,

velocity (and relevant energy), and bouncing heights of falling rocks (Lan et al. 2007).

Remote sensing (RS) techniques have undergone significant and rapid developments in the last few decades. The capability of RS in acquiring very high-resolution terrain contours and 3D spatial data enables effective and advanced investigations of landslide phenomena. The acquired data from multi-sensors (ground and airborne-based data collection techniques) provide useful information for simulation, validation, and model development of natural phenomena (Scaioni et al. 2014). LiDAR technologies are one of the most commonly utilized technologies in landslide research. The emergence of RS and Geographic Information Systems (GIS) has facilitated the application and extension of difference methods and algorithms in landslide researches. Modern insights into landslide studies have been obtained by identifying and mitigating failures using these techniques (Mezaal et al. 2017a, b).

An accurate and high-resolution DEM enables researchers to obtain various useful parameters, such as slope, aspect, curvature, flow direction, and other hydrological

---

✉ Biswajeet Pradhan  
Biswajeet24@gmail.com; Biswajeet.Pradhan@uts.edu.au

<sup>1</sup> Department of Civil Engineering, Faculty of Engineering, Universiti Putra Malaysia, 43400 UPM Serdang, Malaysia

<sup>2</sup> School of Systems, Management and Leadership, Faculty of Engineering and Information Technology, University of Technology Sydney, Building 11, Level 06, 81 Broadway, PO Box 123, Ultimo, NSW 2007, Australia

and terrain parameters. Such parameters are widely utilized in the investigations and mapping of landslides. The high-resolution terrain parameters acquired utilizing LiDAR allows accurate landslide mapping, which can be utilized in landslide susceptibility, hazard and risk assessments. Lately, the LiDAR applications in landslide research have remarkably increased due to accurate terrain data acquisition over wide areas within a short period of time (Slatton et al. 2017).

Rockfall is widespread and can threaten people and their properties, structures and infrastructures, and transportation lines. It is significantly hazardous in hilly and mountainous regions in addition to the artificial excavations along road cuts. Rockfall basically composes of little volume, but is more common on several slopes, and can caused long runout distances. Rockfall protection needs the characteristics of rockfall hazard scenarios, intensity and frequency of impacts, accounting for spatial distribution, cost-efficiency analysis of mitigation measures, vulnerability of exposed elements, and expected costs (Agliardi et al. 2009). Generally, the issue is frequently dealt with through design of engineered mitigation measures (Ritchie 1963; Lambert and Bourrier 2013) or the susceptibility and hazard assessment (Crosta and Agliardi 2003; Frattini et al. 2008).

Rockfall dynamics relies on slope topography, block geometry, surficial geology, and vegetation. Thus, the efficiency of rockfall protections and the reliability of analyses rely on the proper computation for all related methodological problems and on the modeling predictions accuracy. This paper basically explains the principles of LiDAR techniques and the factors that can be derived from the LiDAR point cloud (Pradhan et al. 2017; Yan et al. 2012). It also demonstrates the general methodology and principles of rockfall risk, including rockfall types, triggering factors, mechanism, rockfall sources identification and modelling approaches for rockfall risk assessment.

## 2 Rockfall

Rockfall is a hazardous and frequent process that results from the failure of rock-masses, progressive weathering (Rosser et al. 2013), and is a significant contributor to sediment transport budgets of mountain. Rockfall is initiated when a rock block becomes detached from the rock-mass under the gravity action. Rockfall is distinguished from other movements of mass such as rock avalanches or rock slides (Petley 2013) by its volume, between  $10^{-2}$  to  $10^2$  m<sup>3</sup>, but can be up to  $10^5$  m<sup>3</sup>. Despite the fact that rockfall is classified under the general category of landslide (Table 1), its dynamics are essentially various from rock avalanches and slides, as single boulders and rocks whose movement is governed by discrete ground impact. Instabilities of rock-mass which result in rockfall can pose a serious threat to infrastructure and the mitigation of rockfall is a significant task in all countries with engineered rock slopes or mountainous terrain.

### 2.1 Rockfall Triggering Factors

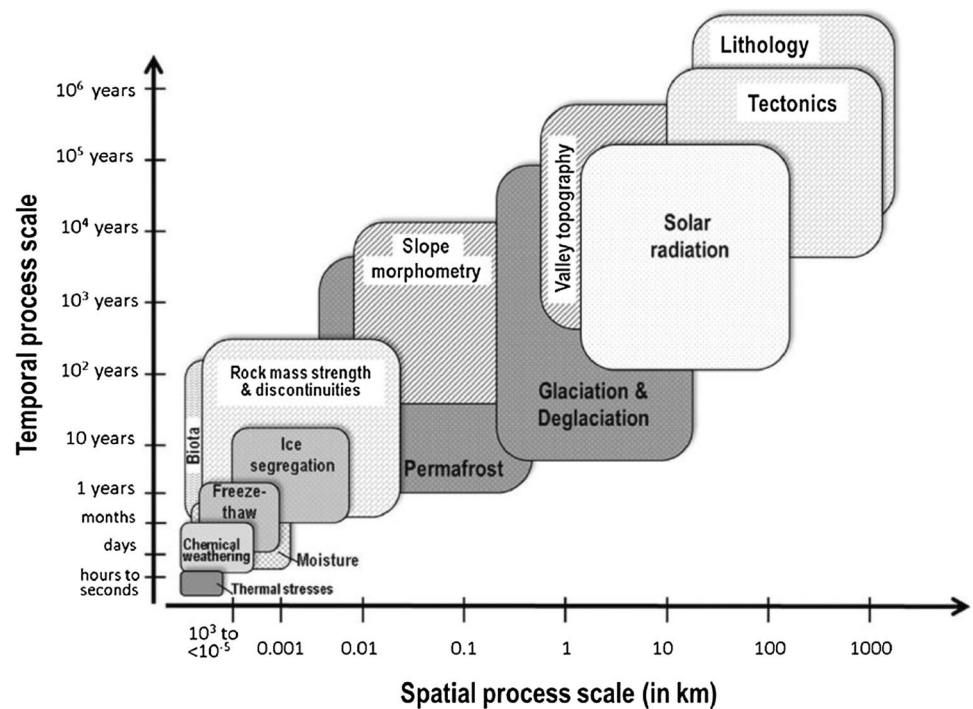
The behavior of rockfall is unpredictable and there are many factors that trigger rockfall along an excavated and/or a natural slope. The triggering factors can be classified into natural process such as rainfall and freeze–thaw, weathering, earthquakes, water seepage volcanism and root wedging. Human activities such as vibrations from machinery and blasting, earthworks that alter slope morphology, deforestation, and more livestock grazing on steep slopes, is considered another rockfall triggering factors (Dorren and Seijmonsbergen 2003). However, the heterogeneous spatial distribution of debris landform within mountainous landscape as well as their variance properties of material and volumes indicates a compound interaction of multiple causal factors, jointly defining the rock-walls sensitivity to fail at various temporal and spatial processes scales (Fig. 1).

**Table 1** Landslide classification scheme (Varnes 1978)

Type of movement	Type of material		
	Bedrock	Engineering soils	
		Predominantly coarse	Predominantly fine
Falls	Rock fall	Debris fall	Earth fall
Topples	Rock topple	Debris topple	Earth topple
Slides			
Rotational	Rock slide	Debris slide	Earth slide
Translational			
Lateral spreads	Rock spread	Debris spread	Earth spread
Flows	Rock flow (deep creep)	Debris flow (soil creep)	Earth flow (soil creep)

*COMPLEX* Combination of two or more principal types of movement

**Fig. 1** Processes-scale of probable rockfall controls with respect their spatial and temporal variability. Adopted from Messenzehl et al. (2016)



## 2.2 Rockfall Mechanics

Rockfall process starts from the release region where boulders are dislodged and move down slope, runout through the transition zone where peak dynamic activity is observed, and the rocks slow and come to a stop at deposit zone (Akgün and Yakut 2017). The size, shape, and release mechanism of rockfalls is governed by discontinuities and fracture of intact rock or failure along joint planes, which is preconditioned by rock structures and their properties within the rock-mass (Leine et al. 2014). Therefore, the rockfalls sizes and shapes can be associated with the specific geological setting in the rock-mass in which they are formed (Fityus et al. 2013). Rock detachment is fundamentally driven by weathering processes such as acting upon the rock-mass. After release, rockfall movement consists of falling or flying, impact and bouncing, rolling or sliding, the runout path and the area affected by rockfalls are identified by the combination of these motion modes. Rockfall movement is affected by various spatially variable parameters including the terrain characteristics and the material properties of the rock itself (Volkwein et al. 2011). These effects can be classified into:

1. The material properties of the rock and terrain: including stiffness, strength and friction (Lambert et al. 2013).
2. The configuration of impact: defined by the combination of rock-shape and size, terrain morphology, in addition to the rock kinematics (rotational and translational velocity) and orientation at the impact point (Volkwein et al. 2011).

3. Vegetation and vegetation density: this is the strength, frequency and size of tree cover in forested regions, along with thickets and bushes (Mezaal and Pradhan 2018).

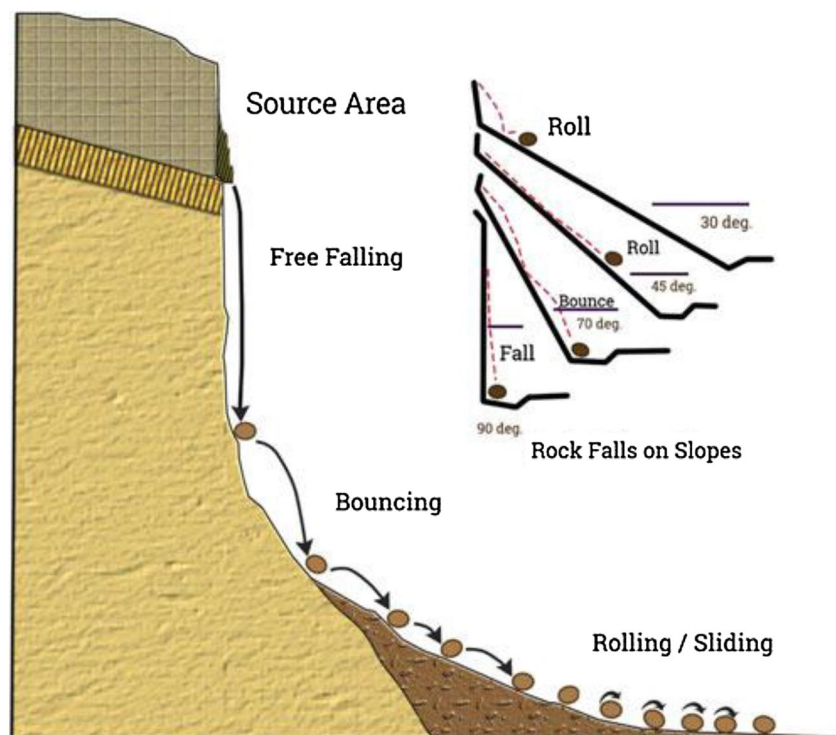
## 2.3 Rockfall Motion Modes

Ritchie (1963) has described the characteristics of rockfalls runout behavior based on the angle of terrain slope, defining four motion modes (Fig. 2). The combination of motion modes from the release point to deposit zone makes the path of a rockfall trajectory. Ritchie's research was one of the first comprehensive research on rockfall behavior according to in situ observation of rocks rolled along roadside rock cuts. His research was intended as an engineering guide for the rockfall catch ditches design.

## 3 LiDAR Technique

In the last few decades, RS techniques have experienced rapid and important developments. The ability of enhanced and modern RS techniques to capture very high-resolution terrain contours and 3D spatial data permits effective and advanced investigation of landslides phenomenon (Pradhan and Yusof 2017). Information obtained from multi-sensors supplemented with ground-based and airborne-based data gathering methods provides functional data for simulation of natural phenomenon, validation, and model development (Fanos and Pradhan 2016). Interferometric

**Fig. 2** Rockfall motion modes related to slope angle (Ritchie 1963)



synthetic aperture radar and light detection and ranging (LiDAR) are two of the most commonly employed techniques in landslides assessment. In comparison with conventional techniques, these methods allow rapid and accurate mapping of geomorphological factors (Roering et al. 2013; Daehne and Corsini 2013). Moreover, the advancement of RS and GIS has simplified the extension and application of different techniques and algorithms in landslides research. Modern insights into landslides studies have been derived through the determination and mitigation of failures by these technologies. Without RS and GIS technologies demands a huge budget to identify landslides-prone areas.

LiDAR is an effective RS data capturing method. LiDAR produces high-resolution Digital Terrain Model (DTM) and its several derivatives such as detailed geomorphological factors. The high-resolution DTM can be in true 3D point clouds, triangulated irregular networks (TINs), or raster grids. An accurate DEM permits users to obtain many valuable parameters, such as slope, curvature, flow direction, and other hydrological and terrain parameters which are widely utilized in landslides assessment (Mezaal et al. 2017a, b). The availability of high-resolution terrain information derived from LiDAR allows accurate mapping of landslides that can be utilized in landslides susceptibilities mapping as well as in hazard and risk analyses. In most recent years, LiDAR applications in landslide research have been remarkably increased worldwide.

### 3.1 System Components

LiDAR is a tool that generates and transmits a pulse series or a beam of collimated, in-phase, coherent, and directional electromagnetic radiation (Pradhan and Fanos 2017a). LiDAR system can be used to collect enormous volume of 3D terrain data at exceedingly rapid recording rates. The laser scanning system can be of many types: an airborne-based laser scanning system (ALS) and a ground-based laser scanning system, terrestrial (TLS) and mobile (MLS), (Fig. 3). The primary processing and concepts of ALS have been known since the 1990s.

### 3.2 LiDAR Accuracy and Resolution

The normal laser instruments accuracy is  $\pm 1.5$  cm within maximum distance of around 700–1000 m. Nevertheless, instrumental accuracy is basically subjected in actual application due to reverse conditions, involving extremely bright ambient setting, poor climate condition (rain, hot wind, and fog), exceedingly uneven or poorly reflecting surfaces, excessive range, and parallel incident angles (Jaboyedoff et al. 2012).

Laser scanner resolution is an element that establishes the extent of the details that can be observed in a point cloud. The resolution is classified into: angular/spatial and range. Angular resolution indicates to the rangefinder capability to address two features on neighboring line of sights. This element is dominated by the following factors: user-defined

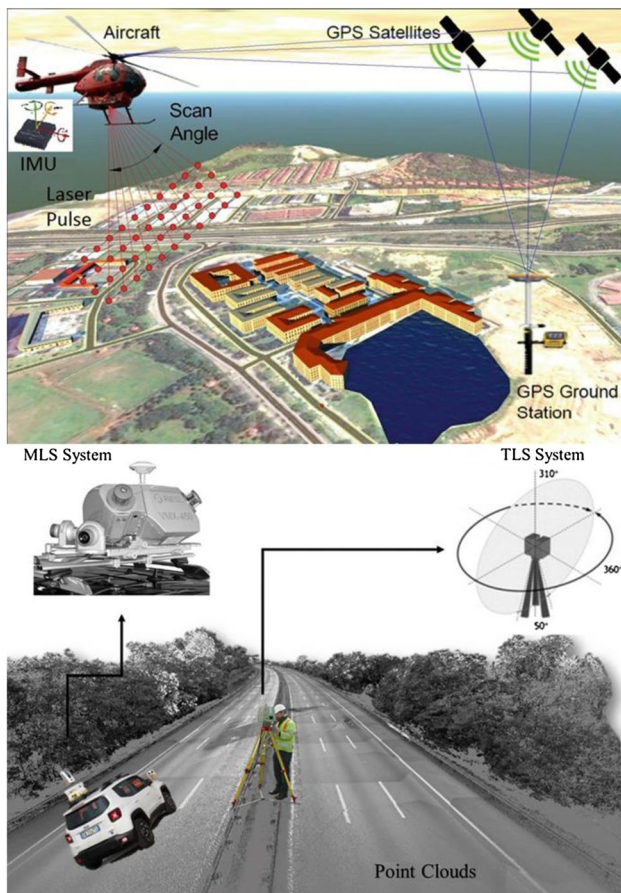


**Fig. 3** Components of typical LiDAR system. Modified after Pradhan and Sameen (2017)

point spacing or sampling interval and the width of laser beam, which is contingent on the distance and the instrument. Range resolution indicates to the rangefinder ability to address two features on the same line of sight. Apart from the location, the reflected signal intensity is derived. This aspect essentially depends on the material type (the color and roughness of the reflecting surfaces), soil moisture, incidence angle, and beam wavelength.

The typical point density of TLS system ranges from 50 to 10,000, whilst of ALS ranges from 1 to 100 pts/m<sup>2</sup> (Jaboyedoff et al. 2012). Despite the fact that, the LiDAR point density is dominated by various elements, involving incidence angle, beam wavelength, soil moisture, and type of target materials. Thus, point density can alter from one region to another for the same instrument.

### 3.3 LiDAR Data Processing Methods

Generally, LiDAR sensors can produce a massive spatial data volume with 3D coordinates within a short period. LiDAR generates uneven points distribution based on configurations and characteristics of a system. Raw LiDAR data

are unorganized, and therefore, GIS systems are required for organizing such massive spatial data amounts. Then, data filtering can be performed to visualize data and to rebuild features (buildings and trees) and bare-earth ground surfaces. The following sections describe the three most significant LiDAR data processing techniques, namely filtering, geometric calibration, and interpolation, to enhance understanding of their usage and concept in the application of landslides (Pradhan and Sameen 2017).

#### 3.3.1 LiDAR Based Digital Surface Model (DSM) Filtering

The filtering of LiDAR data refers to the processes of differentiating non-ground points from ground points of the LiDAR point cloud. The filtering concept is based on the observation that an important height variance between two close points is improbable to be resulted from a steep slope in the topography. The filtering processes are only carried out to derive a digital elevation models (DEMs) or DTMs from a Digital Surface Models (DSMs). Moreover, LiDAR data filtering is needed to reduce computational loads and to optimize data for analysis.

In landslide research, DSM point cloud filtering is not as frequent as the filtering of laser scanning data and it is according to the close-range photogrammetry method (Zhan and Lai 2015). LiDAR-based DSM and DEM is frequently utilized in landslide investigation mainly because of their rapid data acquisition and high-resolution elevation data (Dou et al. 2015; Bui et al. 2016). Nevertheless, several similarities exist between LiDAR and photogrammetry point clouds data filtering techniques. The frequent filtering method, proposed by Kraus and Pfeifer (1998), is an iterative linear least squares interpolation. This algorithm is widely used to generate a DEM for forest areas by removing tree observations from the data of airborne laser scanning. Bornaz and Lingua (2002) has proposed an adaptive TIN method that could handle surfaces with discontinuities. Vosselman (2000) developed a slope-based filtering method whose concept depends on the assumption that the slopes of non-terrain features (buildings and trees) would be obviously various from the slope of a natural terrain. This algorithm has been improved by Sithole and Vosselman (2001) through utilizing a slope adaptive filter. Another method was proposed by Zhang et al. (2003) for removing features utilizing slowly increasing window size, which could adequately eliminate most non-ground points. In another paper, Jahromi et al. (2011) has presented a new filtering method based on artificial neural network (ANN) to derive bare-earth points from ALS data and accurately produce a very accurate DEM for urban areas. In a recent paper, Zhan and Lai (2015) proposed a novel method for DSM filtering to monitor the landslides. This method was presented to resolve the issues of

noise points and vegetation interference in DSM filtering for the monitoring of landslide.

Multiscale curvature classification (MCC) is a repeated multiscale method to classify LiDAR returns that override the thresholds of positive surface curvature, that result in all the LiDAR observations being classified as non-ground or ground (Evans and Hudak 2007). This algorithm donates a classified returns solution that assist the interpolation of bare-earth surfaces at a resolution corresponding with the LiDAR sampling frequency surveying. The MCC algorithm provides high confidence in the obtained ground surfaces and minimizes commission errors while retaining a high proportion of ground return (Evans and Hudak 2007).

### 3.3.2 Registration

Point clouds registration is commonly a Euclidean transformation process that combines rotation and translation according to a coordinate system and a reference point. Normally, the point clouds acquired from various locations should be accurately registered before data processing to confirm optimization of the data. LiDAR point clouds registration is basically conducted utilizing three major techniques: point-to-point, feature-based, and target-based techniques (Abellán et al. 2014). The first method is basically based on the gradually distance minimization between identical points in two overlapped point clouds. Point-to-point method is frequently utilized in the applications of geoscience; nevertheless, a large number of iterations may be needed (Abellán et al. 2014). Effective algorithm should be used in this method to generate beneficial products that can be employed in the investigations of landslide. Deformation in the geometry of surfaces may result in less accurate slope information. In feature-based method, pipelines and power lines are normally identified and utilized for registration process (Chen et al. 2017). Such methods are widely used in industrial applications and seldom in landslides research, because the distinctive geometric characteristics are rarely presented in complex rock slopes. The third methods utilize a precise survey by total station or GNSS techniques. These methods are tedious and time-consuming and demands additional instruments. However, many researchers have examined these approaches on the monitoring of landslide and derived satisfactory outcomes (Abellán et al. 2014).

### 3.3.3 Geometric and Radiometric Calibrations

LiDAR data geometric calibration aims to eliminate systematical error from point clouds. This error in LiDAR data are essentially resulted from the biases in mirror angles and measured ranges and biases in parameters relevant to system components (boresight angles and lever arm) (Zhang et al. 2013). Data driven (strip adjustment) and system driven

(calibration) are the two major methods for elimination of systematic error. Calibration techniques are according to the physical sensor models that relate the parameters of a system to the ground coordinates of LiDAR points. In contrast, the data-driven method basically uses mathematical model that relates the reference frame and LiDAR strips (Zhang et al. 2015). Systematic error influences the parameters of the system are mainly modeled by an arbitrary transformations function between the reference frame coordinates system and the laser strip. In the research performed by Habib et al. (2011), magnificence enhancement in vertical and horizontal accuracies was proven after eliminating the evaluated biases impact in the parameters of a system.

The LiDAR data radiometric correction aims to eliminate the impacts of laser energy attenuation resulted from object surface backscattering and atmospheric effects (Yan et al. 2012). This correction can be carried out utilizing physical and empirical methods. The empirical method does not take into account the physical properties of the laser backscattering energy. The intensity of LiDAR has been utilized to study the structure and geomorphology of active landslide bodies and volcanic surfaces. Fornaciai et al. (2010) noted that lava flow, sediments, air fall deposits, and vegetation revealed distinguishing LiDAR intensity response. Yan et al. (2012) stated that the radiometric correction of LiDAR intensity data could remarkably enhance the land cover classifications accuracy. Land cover data are commonly required for the classification of landform and is generally used in landslides research. Wang et al. (2013) noted that LiDAR intensity was highly beneficial in identification of landslide boundaries. According to the above-mentioned literature review, the radiometric correction intensity data is anticipated to enhance more accurate geomorphic features in the applications of landslides than raw intensity data acquired utilizing LiDAR sensor.

### 3.3.4 Interpolation

DEM can be represented as triangulated irregular network (TIN) or raster images. Apart from TIN-based DEM, interpolation is needed for transformation of scattered ground points to grid based DEM. The main interpolation techniques are the probabilistic and deterministic techniques (Chen et al. 2017).

Probabilistic method hypothesizes that there is a set of fixed values for an un-sampled position and a random variable for each position. While the predicted values are appointed to the un-sampled positions, the occurrence probability can be also calculated. Such methods work effectively when the point density is low or prior knowledge is missing. The typical probabilistic techniques are Kriging, linear prediction, and conditional simulation (Ashraf et al. 2017). These techniques utilize the variogram for estimating of

the missing values. By interpolation, the study area spatial variation is considered in detail. Thus, these methods type is more likely to be generalized. In addition, the estimated value uncertainties give researchers some key reference on the results reliability. Nevertheless, the linear prediction method (mathematically similar to Kriging method) and Kriging may result in the loss of some terrain details and the smoothing effects while the conditional simulation may lead to massive estimation error.

Deterministic methods consider the estimated values of un-sampled regions as the real values without any uncertainties. Such methods are efficient when the physical mechanic is known and sampling points are densely distributed. If the physical mechanic is unknown or sampling points are sparsely distributed, it is improper to neglect the estimation errors. The commonly utilized deterministic methods are Radial Basis Function (RBF), Inverse Distance Weighted (IDW), and Trend Surface (TS).

### 3.4 LiDAR Data Products Used in Landslide Modeling

The mapping and chosen of a proper set of conditioning factors correlated with landslides incidents demand a prior knowledge of the major contributors of landslides. The most frequent landslide conditioning factors that can be obtained from LiDAR-based DTM are altitude, slope, curvature, aspect, topographic wetness index (TWI), sediment transport index (STI), topographic roughness index (TRI), and stream power index (SPI). The following subsections present each of these conditioning factors obtained from LiDAR-based DTM (Pradhan and Sameen 2017).

#### 3.4.1 Altitude

Generally, LiDAR techniques are utilized to derive very high-resolution DEMs and DSMs. The present accessibility of DEMs obtained utilizing LiDAR sensors allow improving of landslides identification and mapping. In addition, LiDAR technique has a greater advantage of being capable to penetrate vegetation canopies and result significant information about the terrain topography (Slatton et al. 2017). Due to this ability, LiDAR data can be distinguished in comparison with other sources, such as photogrammetry, in revealing landslides and scarp areas in forested regions. According to the literature, LiDAR-acquired DEM is mainly utilized for the semiautomatic identification of landslide characteristics and the visual evaluation of topographic surface. Ardizzone et al. (2007) stated that the using of LiDAR-acquired DEM can improve the detection of landslide locations in comparison with analyzing aerial photographs.

#### 3.4.2 Slope

Slope refers to the change in elevations. It is considered one of the major landslides conditioning factors utilized in almost every landslides susceptibilities studies. Slope is a significant factor in landslides research due to its correlation with the driving gravitation force. Generally, slope angle has a positive linear correlation with landslides incidents. That is as the slope degree increases the gravity vertical component increases as well. The calculation of slope can be performed through 3D grid data obtained utilizing LiDAR or other traditional techniques. However, the slope can be accurately derived utilizing specific mathematical algorithms because LiDAR gathers high-resolution elevations information that can be represented in a grid format. The neighborhood algorithm is one of the most popular techniques proposed for the calculation of percentage of slope (Zeng et al. 2017). It calculates slope for each cell in an elevation grid through analyzing every  $(3 \times 3)$  neighborhood cells. Slope degree can be obtained through the conversion of slope percentage afterward. Figure 4 illustrates the major stages for slope computation from LiDAR point cloud.

The triangle in Fig. 4c is utilized to compute slope from an interpolated grid. Slope is defined by the vectors  $(S_1, S_2)$ ,

$$S_1 = \frac{z_0 - z_1}{d_1} \quad (1)$$

$$S_2 = \frac{z_1 - z_2}{d_2}. \quad (2)$$

In which  $z_i$  denotes the elevations between pixels and  $d_i$  denotes the distances between pixels, as illustrated in Fig. 4c. Then slope magnitude and direction is calculated as below:

$$S = \sqrt{S_1^2 + S_2^2} \quad (3)$$

$$r = \tan^{-1} \frac{S_1}{S_2} \quad (4)$$

in which  $S$  is slope magnitude,  $r$  is slope direction, and  $(S_1, S_2)$  are vectors that represent the downward slope.

Chow and Hodgson (2009) analyzed the impact of LiDAR post-spacing and DEM resolution on the estimation of slope mean. Their analysis revealed that the variation between modeled slope mean and slope mean decreased with increasing spatial resolution and point density of DEM. They noticed that the relation of the slope mean with different post-spacing and cell size suggested a linear and a logarithmic function, respectively, for all research regions. In addition, cell size had a more important impact on the slope mean than the posting densities of LiDAR. Moreover,

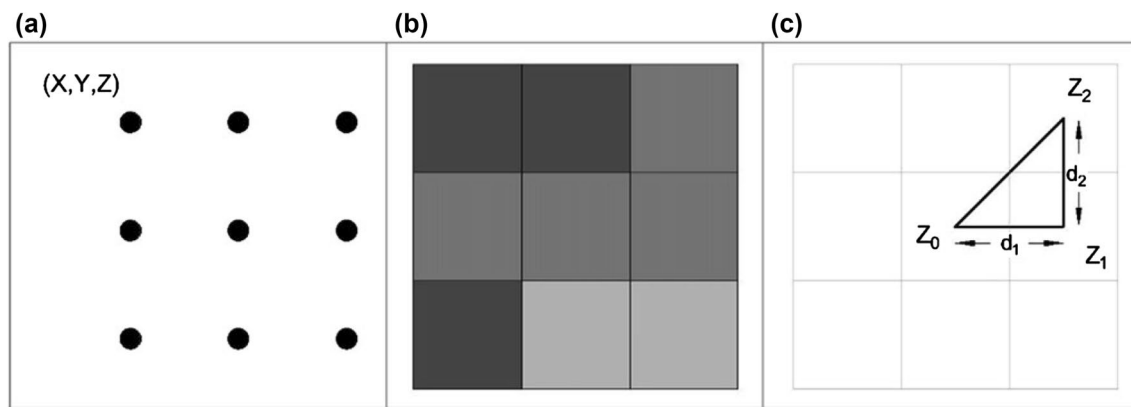


**Fig. 4** Main steps for slope calculation. **a** An example of LiDAR point clouds, **b** interpolated grid, and **c** definition of variables for calculating slope on a single facet (Pradhan and Sameen 2017)

their research also suggested that interpolation techniques and their parameters considerably influenced the generation of DEM, and subsequently, other derivatives such as slope, aspect, and curvature.

In another paper, Chen et al. (2016) performed a research on the relation between slope angle and landslide size. Their findings revealed that as slope angle increased, potential slide size or sliding mass volume decreased. In contrast, another research based on numerical simulation carried out by Katz et al. (2014) suggested that more material could fragment for a specified material strength in steeper slope, and thus, the produced landslides could be bigger. Such contradictions suggest that considerable controls for slope angle affect the landslides size for a particular material strength.

### 3.4.3 Aspect

Slope direction or aspect specifies the downslope direction of the maximum change rate utilizing eight neighboring cells and subsequently, defines the flow direction. In some areas, patterns of soil variances are relevant to the aspect variations. Slope aspect controls the landslide formation, such as rainfall, lineaments, exposure to sunlight, and wind effects. Therefore, aspect indirectly affects landslide and has been utilized in considerable studies of landslides susceptibility mapping. The generation of aspect maps is based on the compass direction that a surface faces at raster cell position. The measurement of aspect is clockwise and coming full circle from 0 (due north) to 360° (due north). A value of -1 is given to the flat areas with no downslope direction. Figure 5b illustrates an example of an aspect map obtained from high-resolution LiDAR-based DTM. In this example, aspect values keep increasing which indicates that the compass direction computed utilizing the ESRI algorithms. Although, in landslides studies an aspect map is normally

categorized into nine classes namely: north, northeast, east, southeast, south, southwest, west, northwest, and flat.

### 3.4.4 Curvature

Basically, curvature defines as the change rate in aspect or slope degree and has been reported to influence slopes failure. Through utilizing a general curvature map, the flow and slope morphology characterization can be assessed (Nefeslioglu et al. 2008). Profile curvature, which is the perpendicular plane parallel to the slope direction, influences the deceleration and acceleration of downslope flow, and thus, affects erosion and deposition (Kritikos and Davies 2015). The plan curvature is identified as the curvature of a contour line found by the crossing of the surface with a horizontal plane. It affects the divergence and convergence of flow along a slope. Moreover, Fernandes et al. (2004) stated that curvature could be affected by slope erosion processes, such as the divergence or convergence of water during downhill flows. In addition, curvature is considered as one of the landslide-related factors that control landslides incidents.

### 3.4.5 Hydrological Factors

Adding to morphological factors, landslide is controlled by many hydrological factors, such as TWI, SPI, STI, and TRI. TWI is defined as a steady state wetness index. It is frequently utilized to account topographical control on hydrological processes and is a function of both flow direction and slope. In addition, TWI is another topographic factor within the runoff model and it characterizes the impact of topography on the size and location of saturated sources regions of runoff generation. TWI is expressed as bellow:

$$TWI = \ln \left( \frac{A_s}{\beta} \right). \quad (5)$$

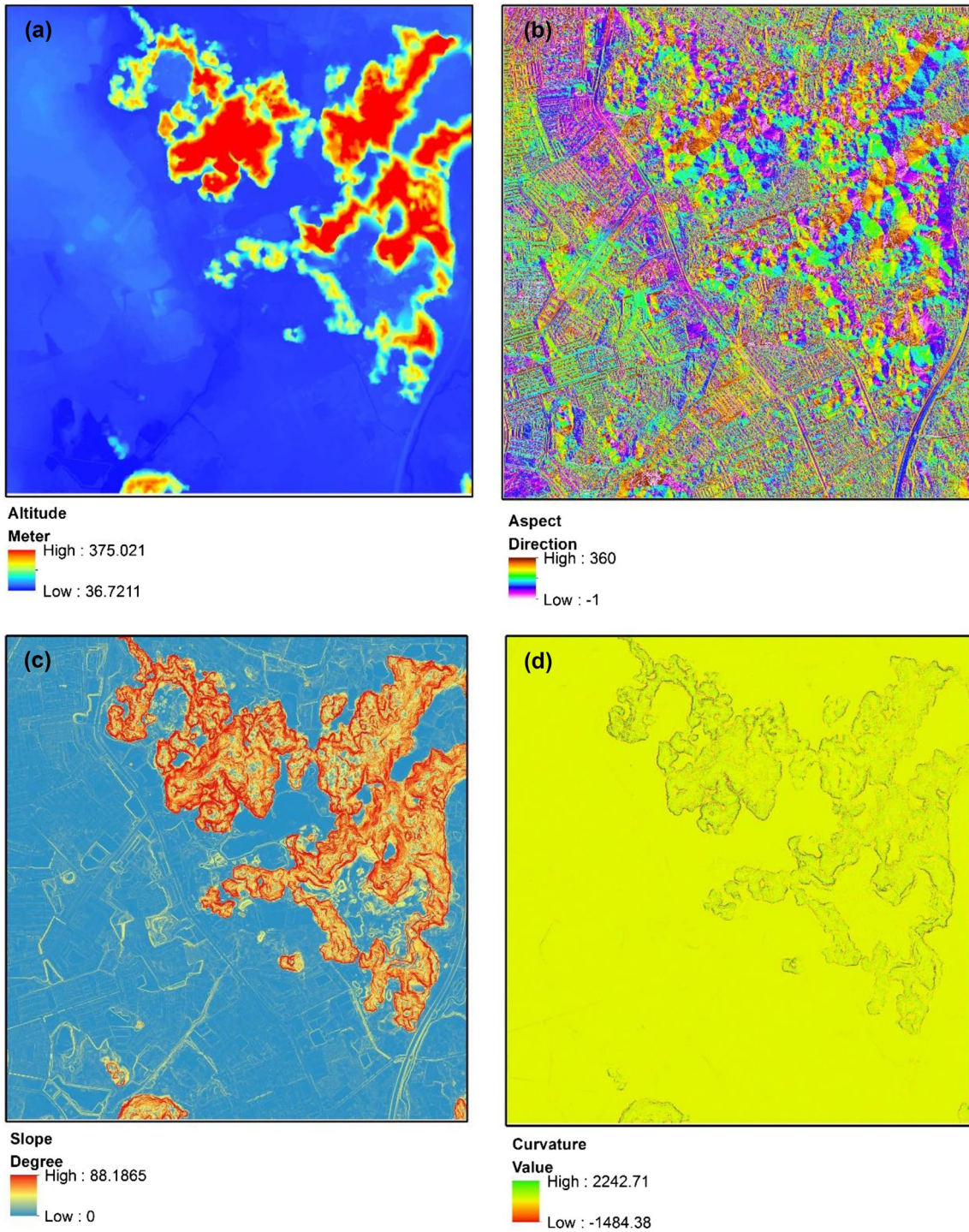


**Fig. 5** Examples of geomorphic parameters derived from LiDAR data. **a** Altitude, **b** aspect, **c** slope, and **d** curvature

In which  $A_s$  is the particular catchment area ( $m^2/m$ ), and  $\beta$  is a sloped angle in radian. Moreover, TWI is a significant characteristic of DTM that indicates soil saturation.

STI, that indicates the erosive power of overland flows, is obtained by taking into account transport capacity restrict sediment flow and catchment evolution erosive theory.

$$STI = \left( \frac{A_s}{22.13} \right)^{0.6} \left( \frac{\sin \beta}{0.0896} \right)^{1.3} \quad (6)$$

SPI, a measure of a stream erosion power, is also a factor that contributes to stabilities within study areas (Regmi et al. 2014). SPI is calculated as bellow:

$$\text{SPI} = A_s \times \tan \beta. \quad (7)$$

#### 4 Rockfall Protection Based on Modeling Support

Rockfall results in serious damages to properties and lives. Therefore, the protection of rockfall is a significant concern when defending exposed valuable targets in exposed regions, or when planning the development of new industrial or urban facility and infrastructure. The protection of rockfall involves risk assessment, structural countermeasure designing, and identification of mitigation options (Volkwein et al. 2011). This demands a precise quantification of rockfall boulders size distribution and susceptibility in the probable source regions, dynamic quantities (bouncing height, velocity, and kinetic energy), expected rockfall trajectories, statistical and magnitude variability of involved distribution and kinematic, and intensity of impacts.

#### 5 Rockfall Source Identification

The rockfall sources identification (releasing points) is a main prerequisite to the modeling of rockfall trajectory, since they produce the premier condition of rockfalls paths, the relevant probability of rockfall releasing and propagations to particular target. The identification of rockfall source areas can be performed utilizing many methods, involving: (1) identification of isolated unstable rocks through geo-mechanical and topographical surveys; (2) morphometric approach, based on identifying of the threshold value of slope angle, either obtained from the decomposition of slope frequency distribution or subjective for identifying the rocky cliff regions; (3) statistical or heuristic ranking of selected structural, morphological and lithological descriptor (Fratini et al. 2008); (4) the analysis of spatially distributed rocky slopes stabilities utilizing limit equilibrium approach for toppling failure, wedge, or plane; (5) geomorphological mapping of active or potential sources and past rockfalls evidences through field surveys or aerial photo interpretation (Agliardi and Crosta 2003); (6) monitoring of the spatial distribution of displacements over rocky cliff, as via GBSAR technique. An accurate stability analysis of rocks that can produce individual rockfall demands in-site discontinuities characterization, involving cliff size, persistence, roughness, and joint orientation. Such data were collected through field discontinuities surveying in the past, which is restricted by budget, safety and logistic problems when dealing with huge rocky cliff. Nowadays, range imaging techniques such as

TLS and Digital Photogrammetry permit precise 3D structural and reconstruction assessment of vast rock cliffs even under highly danger condition. These techniques are relied on the rock-mass strength characteristics and the recognition of joint patterns, and they might be assisted by structural assessment based on remote sensing data. The selection of a particular rockfall sources spatial representation influences the results of runout modeling. An appropriate rockfall sources can be represented as point-like to show the well-known release points or source locations or for back-analysis processes. Linear sources normally symbolize the top envelope of steepest sector or rocky cliff, and are basically relevant to the highest drop height, first impact energy, highest rock potential energy, and fall velocity. Thus, the envelope of cliff-top basically provides the most conservative method for countermeasure design and hazard analysis, beyond a safe method to decrease the number of rockfall source locations deemed for trajectory modeling.

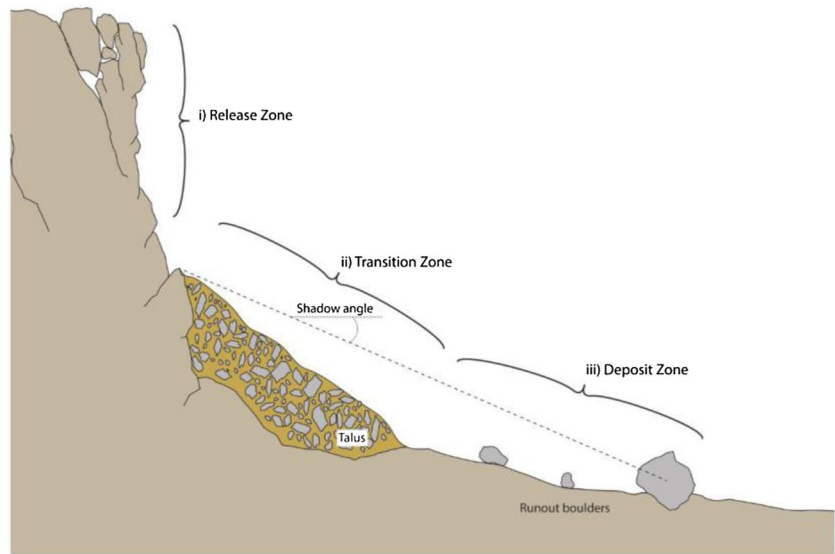
#### 6 Rockfall Simulation Models

The task of modelling rockfall has the ultimate goal of generating rockfall susceptibility and hazard intensity maps (Frattini et al. 2008), and are strongly based on trajectory modelling (Dorren 2016). The quality, reliability and detail of the information available on such models are greatly dependent on the type of model and indeed the complexity with which the rockfall runout process is modelled (Kavzoglu et al. 2014; Peng et al. 2014; Pradhan et al. 2017; Yan et al. 2015).

##### 6.1 2D Rockfall Models

The horizontal 2D approach is the simplest rockfall modelling approach in which the potential areas affected by rockfall is evaluated via assuming a uniform friction for the hazard region, and is carried out through one of two methods (Akgün and Yakut 2017). The first one is to assume that the boulder motion mode is just sliding. This includes the implementation of a regional topographic-hydrological assessment with a sliding friction assumption. This utilizes nearest neighbor process implemented in GIS and finds the steepest decent path along terrain from the source area. The other method is the rockfall energy line approach also known as the travel angle (Evans and Hungr 1993). This method projects a line from the rockfall source area to the farthest accumulate (Fig. 6). Travel angle method considers the detachment location from the top of a rockfall sources, whilst the shadow angle methods project the line from the base, and consider the assumption that rockfall lose 75–85% of its energy through the first impact with the slope surface. The line angle is taken with respect to horizontal and

**Fig. 6** Rockfall activities zone (release, translation and deposit zone) (Evans and Hungr 1993)



is usually chosen according to recorded rock runout length in the study area. Further information related to the predicted kinetic energy along the shadow angle region can also be expected via utilizing the potential height between the energy line and the topography (Fig. 6). The advantage of horizontal 2D methods is that they are capable to make a rapid and broad scale evaluation of rockfall hazard, and can be easily implemented in GIS. In addition, some models offer this as an individual software, such as ConeFall (Jaboyedoff and Labiouse 2011).

Performing rockfall simulation along a 2D vertical topographic profile is the second approach of rockfall assessment that usually select the path of steepest decent as a critical profile section (Van Dijke and van Westen 1990) or an expert defined slope profile, on which a set of ground impacts and their flying stages are simulated. Several rockfall models employing the vertical 2D method are listed in Table 2. The variances among these models are reflected in their approach to modelling the ground impact of the rock. Such approach is restricted in the prediction of the rockfall lateral spread. Nevertheless, runout distances, bouncing height, translational velocity and in some cases angular velocities and contact forces can be calculated for a 2D profile.

## 6.2 2.5D Rockfall Models

The 2.5D model is basically the composition of the vertical and horizontal and 2D modelling approaches. First horizontal 2D simulation is carried out to specify the steepest decent path producing the 2D vertical profiles for the modelling of trajectory; Rocky3 (Dorren and Seijmonsbergen 2003), is an example of this model. Such models supply some information of the kinematics of rock along the spreading region.

However, these models do not account for the rock potential to diverge from its path because of the rock-shape or terrain morphology, and thus the lateral spreading are nor accounted.

## 6.3 3D Rockfall Models

The 3D rockfall model computes the vector of rock position in three dimensions with varied detail degrees. The major advantage of 3D over 2D models is that 3D model is capable to account for the terrain morphology impacts and can calculate trajectories divergence. The list of existing rockfall models and their abilities is given in Table 2, updated from Li and Lan (2015). The major variances between 2D and 3D models can be observed in how the boulder is modelled.

1. Rigid body model takes into account the rock geometry, this can be ellipsoids, arbitrary polyhedral, or a simple rectangular rock. The block is given a mass for which the mass center is tracked in relationship to the rock and its inertia tensor. Thus, this approach permits the location vector of the simulated block to be determined alongside with its direction that is usually defined with a quaternion, consequently the vectors of location, angular and translational velocity are specified. This approach takes into account the full gyroscopic forces and enables the forces to be computed at obvious touching points on the body of the block. This allows the study of the block geometry impact on the characteristics of trajectory. The boulder is considered unbreakable and rigid. Thus, the fragmentation influences and the deformation of body because of the applied forces are not considered. Nevertheless, the approach is more numerically adequate in compression with discrete element method, and along

**Table 2** Existing rockfall simulation models

Program name	References	Spatial dimension	Simulation approach
N.N	Ritchie (1963)	2D (slope profile)	Lumped mass
Discrete element method	Cundall (1971)	2D (slope profile)	Rigid body
Computer rockfall model	Piteau and Clayton (1976)	2D (slope profile)	Lumped mass
ROCKSIM	Wu (1985)	2D (slope profile)	Lumped mass
SASS	Bozzolo and Pamini (1986)	2D (slope profile)	Hybrid
N.N	Hungr and Evans (1988)	2D (slope profile)	Lumped mass
Rotomap	Scioldo (1991)	3D (x, y, z)	Lumped mass
CADMA	Azzoni et al. (1995)	2D (slope profile)	Hybrid
STONE	Guzzetti et al. (2002)	3D (x, y, z)	Lumped mass
Rocky3	Dorren and Seijmonsbergen (2003)	2.5D (x, y coupled with slope profile)	Hybrid
HY-STONE	Crosta et al. (2004)	3D (x, y, z)	Hybrid
Rockyfor	Dorren and Berger (2006)	3D (x, y, z)	Hybrid
RockFall analyst	Lan et al. (2007)	3D (x, y, z)	Lumped mass
RAMMS:Rockfall	Christen et al. (2007)	3D (x, y, z)	Rigid body
PICUS-ROCKnROLL	Woltjer et al. (2008)	3D (x, y, z)	Lumped mass
PICUS Rock 'n' Roll	Rammer et al. (2010)	3D (x, y, z)	Hybrid
Rockyfor3D	Dorren (2012)	3D (x, y, z)	Hybrid
NURock	Spadari et al. (2013)	2D (slope profile)	Lumped mass
RocFall	Rocscience Inc. (2013)	2D (slope profile)	Hybrid
RAMMS:ROCKFALL	Leine et al. (2014)	3D (x, y, z)	Rigid body
RocPro3D	RocPro3D (2014)	3D (x, y, z)	Hybrid

with the personal computer advance, computation time can be less than 1 s per trajectory.

- Point-mass model considers the whole block-body as a point-like particle. This model neglects the geometry of boulder and the interchange of energy between translational and angular velocity. The computation of kinematic information includes translational velocity and location vectors.
- Discrete element method, models a block-body as a combination of small mass-points or spheres that are linked via elastic elements. Thus, rock deformations can be predicted, providing criterion to fragment and break.
- Sphere model considers a boulder as a rigid sphere with a set radius. This allows the rocks inertia moment and mass to be calculated along with the vectors of location, angular and translational velocity. However, the issue with utilizing spheres is that they will roll over all inclined surfaces, and thus usually over predict runout and must, therefore, use threshold values to stop the modeling.

## 7 Rockfall Parameters

Once the rock released from the rock wall, its falling behavior is controlled by rock and slope properties and slope geometry (Fanos and Pradhan 2016). Spherical-shaped rocks and bare hard rock slope with a smooth surface represent the most considerable rockfall hazard. The parameters of slope properties which affect rockfall trajectory are as following:

- Coefficient of restitution: the retarding capability of the slope surface is the most significant parameter affecting the behavior rockfall. Tangential and normal coefficients of restitution are utilized in the analysis of rockfall.
- Surface roughness: the slope surface irregularities account for most of the variance recorded among rock-falls because they vary the angle at which a block hit the slope. The slope roughness is defined as the maximum vertical variance within a slope distance equal to the rock radius, or the slope angle variation from the average angle of this slope.
- Rolling friction coefficient: the slope resistance to the rock angular velocity, defined as the angle tangent at which a rock initially at rest starts rolling.
- Coefficient of friction: the slope resistance to the rock sliding, defined as the angle tangent at which a boulder initially at rest begins sliding.

## 7.1 Calibration of Model Parameters

Mostly the parameters in rockfalls trajectories simulation are semi-empirical or empirical, and give a convergent phenomenological account of complicated physical process. The real rock movement succession over a particular trajectory is seldom known, and many combinations of these motion modes might produce the similar measured trajectory (Agliardi and Crosta 2003). Thus, it is hard to know initially which movement mode prevails in a particular slope segment. This is crucial, due to the various movement sequences could result in various trajectories, bouncing height, and spatial patterns of velocity, even when they have the same maximum runout. Therefore, several calibration restrictions as feasible are in demand to derive the best rockfall dynamic approximation. The frequently utilized calibration approaches in specific rockfalls protections assessment are according to the back-analysis of recorded events or inventory data (Agliardi and Crosta 2003).

The calibration of a model is difficult and time-consuming of the available time for a sound rockfall simulation, even when high-quality data are available. The simplest models are commonly easy to be calibrated, but may not provide realistic outcomes. In 2D simulation model, it is possible to compare between the simulated and observed runout within a particular slope segment. For instance, a normally utilized indicator of accurate performance of a model is exemplified through the observation that 90% of the simulated rocks stop within a slopes sectors where real rocks accumulated. However, the position and length of these slopes sectors could be carefully selected to permit a meaningful comparison (maximum and minimum rocks trajectory) between modeling results and observations. The same method can be utilized in 3D modeling through computing windows or cells to account the distribution of observed and simulated stopping points and impacts (Crosta et al. 2015). Meaningful results could be derived in this case if can identify the exact rockfalls source areas contributing to model cells. In case multi sources contribute to model cells, that is usually the case in 3D simulation, the number of rocks arrested or impacting in every cell relies on the impact of model resolution, the spatial distribution of surface characteristics, and topographic divergence or convergence (Crosta and Agliardi 2003). Eventually, it must be noted that back-analyses is regularly performed in case of extreme and important incidents, near to worst case scenario. Thus, the calibration of model demands in this case the supposition of a moderate values sets of the parameters which control the modeling. This part considers a fundamental for the evaluation of rockfall hazard and risk.

## 8 Rockfall Modeling Approaches

The location of final deposition of rockfall is strongly influenced by how the blocks behave at each contact point with the slope terrain as it moves downslope (Dorren 2016). Generally, the different existing models employ various mathematical approaches to represent the rock movement. Rocks can be represented as either a rigid body or a lumped mass. Rigid body method considers the rock as a defined fixed volume and shape, accounting for detailed associated rock dynamics (Lambert et al. 2013; Leine et al. 2014). Whilst lumped mass approach considers the rock to be a singular dimensionless point (point mass), and do not consider either the rock dynamics such as rotation or the rock-shape (Volkwein et al. 2011).

Almost all the models adopt the coefficients of restitution to represent the rocks rebounding/bouncing, and friction coefficient to determine rolling and sliding. Several publications detailing parameter quantification and calibration of the coefficients of restitution for different study areas (Wyllie 2014; Volkwein et al. 2011). Because of the local terrain variability, a probabilistic approach is normally utilized for varying parameters (both normally and tangentially), within a limit to account for the rock bouncing stochastic nature (Volkwein et al. 2011).

## 9 Rockfall Protection Structures

Rockfall protection structures are an essential tool to mitigate rockfall hazard. Since some of the early works on the processes of rockfall and protection structure design (Ritchie 1963), attempts have been made to provide engineers with rock slope specific design guidelines for protection measures. The variety in rockfall protection solutions available are typically designed with the purpose of halting or deflecting rockfall from its path, and to withstand the expected or modelled impact energy derived from rockfall modelling (Fig. 7).

### 9.1 Rockfall Barriers

Rockfall barriers are structures made up of steel wire netting supported by posts and foundations (Wendeler et al. 2017). Nets are suspended with guide ropes which contain brake elements which plastically deform under load along with the netting. Through this process the impulsive forces of rockfall can be spread over time and reduce the loads in the retaining structure. Such approaches are widely applied as standard rockfall mitigation measures. Rockfall

**Fig. 7** Rockfall barrier systems and their energy rating (ASTRA 1998)

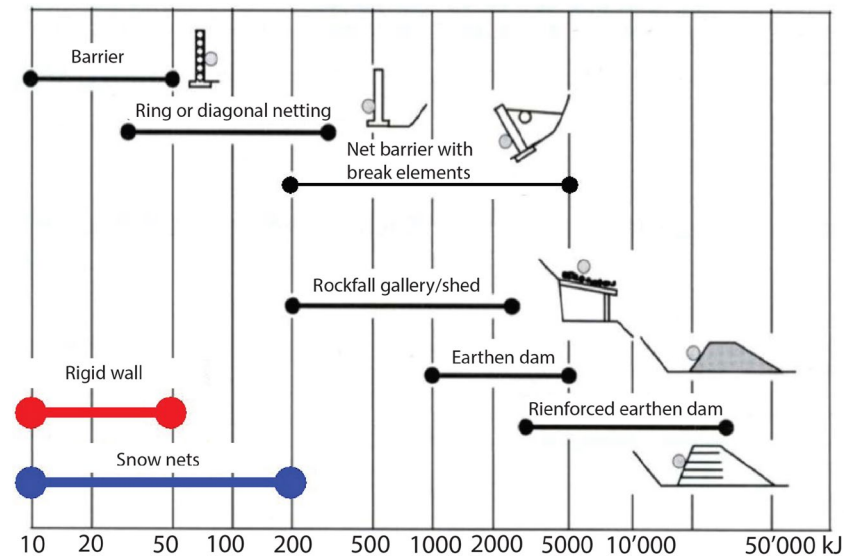


**Fig. 8** Flexible rockfall barrier being impacted by rocks

netting design is supported by rigorous testing procedures and guidelines for their construction. While the testing of rockfall barrier systems is restricted to a standardized rock-shape (Fig. 8), this standardization omits the possibility to observe the effects of angular sharp rocks which would deliver a much greater punctual loading that has yet to be fully investigated.

## 10 Rockfall Conditioning Factors

The prediction of future rockfall to generate hazard and consequently risk maps demand accurate spatial presentation of conditioning factors (Fanos et al. 2016). Realizing the characteristics of the study area and the failure types facilitates the optimal and accurate chosen of conditioning

factors. Several researchers have utilized only few conditioning factors. The major conditioning factors which can be utilized in the studies rockfall are illustrated below:

- *Altitude map* is basically utilized to derive information on different geomorphology factors like slope angle and aspect, surface curvature, flow accumulation, flow direction, and surface roughness. The resolution of DEM limited by data availability, and appropriated to the context of a given kind of assessment. The slope angle strongly influences the stability of a slope. While the slope aspect highly influences hydrological processes through evapotranspiration. The most important factors in the process of the mass movement generation is the elevation. However, elevation alone cannot be utilized for rockfall detection.
- *Geological map* is utilized to derive information about the discontinuities, the type of rock, weathering profile depth, distance from active faults, slope angle relationship, and geological structure. In addition, factors like thermal stress, salt weathering, and frost friction also can be obtained from this conditioning factor.
- *Geomorphology map* is utilized to derive information on slope facets, genetic classification of main landform buildings process, and geomorphological units.
- *Land use map* is utilized in the normalized difference vegetation index (NDVI) or mapping the types of vegetation and the distance from the road. Slope stability can be increases by dense vegetation through two ways: it provides root network which function as a coherence bond for the particles of soil and aids removing soil moisture via evapotranspiration.

## 11 Rockfall Hazard

Within rockfall framework, the hazard of rockfall indicates to the rockfall occurrence probability of a given intensity (energy) or magnitude (volume) within a particular region (Hungar and Evans 1988). The definition involves the position concepts (in which a rockfall incident will happen), magnitude or intensity (energy amount), and frequency (its temporal recurrence) (Pradhan and Fanos 2017b). Consequently, the simplest map of hazard of rockfall should explain the rockfall occurrence probability of a given magnitude within a particular region (Crosta and Agliardi 2003). Due to the speed mobilities of rockfall incidents, the propagation component must also be considered in the assessment of rockfall hazard. Thus, rockfall hazard is basically recognized based on three elements (Volkwein et al. 2011; Crosta and Agliardi 2003):

- Rock detachment probability from the cliff: the rockfall event probability of a particular magnitude (size of rock) happens at a particular sources position along a particular time period. This parameter includes both the probability of spatial occurrence (susceptibility) and the associated temporal probabilities, which is also known as the failure probabilities (frequencies).
- Down-slope propagation: the maximum runout and trajectory of falling rocks.
- Intensity (kinetic energy) of rockfall.

Hence, any assessment technique of rockfall hazard should take into account the rockfall runout and distribution, frequency, susceptibility, and intensity at each position and over the trajectory. Nevertheless, just a few methodologies of rockfall hazard analysis fulfill all of these demanding.

### 11.1 Rockfall Susceptibility

Susceptibilities are the likelihood of occurrence of an incident in a particular region according to the local terrain conditioning factors (Brabb 1984). It delineates the predisposition of a region to be influenced by a particular future incident and provides an estimation of where rockfall is probable to happen (Volkwein et al. 2011). Many techniques have been proposed in the previous studies to delineate the location of potential rockfall incidents.

Susceptibility can be estimated through:

- Deterministic methods.
- Geomorphological mapping utilizing direct and qualitative techniques.
- Statistical analyses (Frattini et al. 2008).
- Empirical and semi-empirical rating methods.

The resulting susceptibility map illustrates the predisposition towards a slope or region instability (Van Westen et al. 1997).

### 11.2 Frequency

Adding to the susceptibilities, the failure temporal probabilities should be assigned to specify the likelihood of the rockfall occurrence. It can be expressed in terms of the return period (known as the frequency reverse) or the frequency of occurrence. The rockfall temporal probability with a particular volume should be analyzed via the statistical evaluation of previous incidents that have happened within a site.

The analysis of in situ-specific rockfall inventory is most commonly utilized method for the rockfall frequency estimation is which provides historical information of time and volume of each rockfall incident. Based on these observations a frequency relation of the magnitude-cumulative can be structured to assess the annual rockfall incidents frequency in particular volume. In case of the lack of historical rockfall incidents, the return period or the frequency are impossible to be precisely evaluated; thus, just the susceptibility of rockfall can be assessed.

### 11.3 Propagation

The rockfall propagation is relative to the falling rock runout (trajectory) along its motion downslope. Basically, the trajectory relies on the features of both the slope and the rock, including the slope roughness, the material of outcropping, the slope topography, the starting location of the rock, its shape and mass, and vegetation density. Many techniques have been stated in the previous studies for the evaluation of the rockfall propagation, and they can be categorized into two major types:

- Physical-based approaches: these approaches depend on numerical simulations (kinematic modeling) for the describing or rockfall movement and propagation accurately. The numerical model considers the rocks as either objects with a defined shape (rigid-body models), or a point (lumped mass approaches), or combining both of them (hybrid body models). The use of numerical simulation is normally for quantitative assessment at site-specific scale.
- Empirical methods: these methods are simple and allow a quick and preliminary evaluation of rocks propagation without utilizing numerical simulation. Empirical method is normally according to the empirical relationship between the runout zone length and the topographic factors. The shadow cone angle method and the “Fahrböschung”, also known as the travel angle (Evans and

Hungr 1993), are the most common methods. These methods permit the estimation of the maximum expected rock runout. The former, that also has been performed in the GIS (Conefall tool), it is also taking into account the kinetic energy. These essential methods are normally utilized where the hazard zone covers a wide region (local and regional and scale).

## 11.4 Intensity

Generally speaking, the assessment of the hazard demands the rockfall intensity of a particular magnitude (volume) to be estimated. Mostly, the intensity of rockfall is defined via the falling rock kinetic energy (Crosta and Agliardi 2003). This is a compound function that relies on the velocity and mass and is determined based on the adopted physical standard.

## 12 Rockfall Risk

Many assessment techniques of rockfall hazard combine risk and hazard evaluation factors. Thus, this section presents many essential concepts that are relevant to the rockfall risk determination. Based on Corominas et al. (2014), rockfall risk is defined via three essential elements: hazards, exposure of the elements at risk, and their vulnerabilities (Eq. 8). These are described via both non-spatial and spatial attributes:

$$Rs = P(M_i) \times P(X_j/M_i) \times P(T/X_j) \times V_{ij} \times C. \quad (8)$$

In which  $P(M_i)$  is the occurrence probability of a magnitude landslides  $M_i$ ,  $P(X_j/M_i)$  is the probability of the landslide accumulated at a location with an intensity  $j$  of a distance  $X$  from the sources of landslide,  $P(T/X_j)$  is the element probability being at the location  $X$  at the time of landslide occurrence,  $V_{ij}$  is the vulnerability of the element to a landslide of intensity  $j$  and magnitude  $i$ , and  $C$  is the value of the element at risk.

The exposure is defined via the temporal and spatial probability that the element at risk is situated at the place influenced via the threat (dangerous) at the occurrence period. The elements at risk location (spatial exposure) incorporate with the rock propagation down the slope (trajectory) specify the reach probability. The reach probability defines the associated rocks frequency that is capable to arrive at particular target positions (elements at risk) along slope surface.

The expected degree of loss is known as the vulnerability and it ranges from 1 (total loss) to 0 (no loss). The vulnerability relies on both the intensity of the threatening incident

that interfaces with it and on the typology of the element at risk (its resistance).

Vulnerability encompasses of four major kinds: physical vulnerability refers to structures and infrastructure, environmental vulnerability refers to the natural environment, social vulnerability refers to the population, and economic vulnerability refers to economic activities.

The usual frameworks for a rockfall risk evaluation comprises of the following stages:

1. Hazard analysis, encompasses the intensity analysis, failure probability and trajectory of the potential rockfall incident.
2. The elements at risk identification, comprising their degree of exposure, value and number.
3. Vulnerability analysis,
4. Risk calculation/estimation.

After the identification of risk, mitigation processes should be applied. Risk mitigation includes applying appropriate management measures and methods and to limit or minimize the effects of hazard and associated disaster.

## 13 Quantitative and Qualitative Approaches

The assessments of rockfall hazard and risk can be either quantitative or qualitative (Fanos and Pradhan 2016). The difference between the two methods is in terms of the input information, employed processes and ultimate results.

Quantitative techniques utilize ranges of values or numerical values alternative to qualitative expressions. This assessment of hazard aims to assess the hazard in the form of numerical probabilities that evaluate the detachment frequencies, encompass intensity and propagation. The quantitative analysis attempts to express the damage and quantify the risk financially. Many recent attempts have aimed to structure standard procedure to quantify risk in terms of official national recommendation or guidelines. Basically, the quantitative assessment of risk has been evolved for quantifying the possible loss probability which are relevant to the hazardous event occurrence via taking into account the number of fatalities, injured persons and destroyed buildings. The tolerable and acceptable risk threshold varies from place to another. The quantitative risk analysis utilizes a reproducible and objective technique to quantify risk and produces absolute outcomes which can be utilized for comparison of various locations, thus providing a fundamental for mitigation measures priority. However, the accuracies of the quantitative risk analysis are varying because they are closely associated with the availability, quality, quantity, and reliability of the data set. The quantitative risk analysis demands many statistical and geo-mechanical information

that restrict its applicability. Therefore, a quantitative assessment may be not much accurate than a qualitative assessment. The accuracy is not relevant to the number of utilizing; rather, it relies on whether the risk and hazard components have been accurately taken into account and on the quality and availability of the information demanded for the rockfalls hazard, vulnerability and exposure assessment.

Presently, quantitative risk analysis is just feasible when a complete inventory data is available of the rockfalls incidents that have happened within the research region. On the other hand, the rockfalls activities documentation is usually absent or poor at most areas, and detailed rockfalls inventory is comparatively rare (Budetta and Nappi 2013), because of the recording lack of medium and small incidents of rockfall. Due to the lack of historical, statistical, and geo-mechanical information which record rockfalls activities, qualitative assessment is frequently utilized techniques. Nonetheless, the major similarities and variations among qualitative techniques have not been explored in the scientific research. Therefore, it is difficult to determine which technique is the best for a particular study area.

Qualitative techniques specify hazard, element at risk and its vulnerability utilizing qualitative descriptors like rating systems, classifications, scoring schemes, weighted indices, ranked attributes, and ranking matrices. Qualitative assessment can be based on either subjective assessment (assumptions or professional judgments), objective (mathematical or statistical) assessment, or combining both of them. The outcomes of qualitative techniques are normally expressed utilizing relative expressions like low, moderate, and high. Mostly, qualitative assessment is more frequently utilized because it is easy to utilize and can be carried out swiftly (Pantelidis 2011). Therefore, most rockfall risk and hazard analysis models are qualitative and employ comprehensive rating to distinguish numerically the risk or hazard at a particular area. The comprehensive rating normally utilizes many parameters to produce a score and/or evaluation for the slopes. Qualitative evaluation produces valuable information for the management of risk and hazard, for facilitating the mitigation measures priority, and for comparative comparisons of various locations. In another word, qualitative evaluation considers a first examination procedure of the predominant hazard at a particular location to assess the riskiest regions further through quantitative techniques.

## 14 Conclusion

LiDAR techniques, including TLS, MLS, and ALS, permit developments in the identification of displaced materials and landslide scarps and the geological mapping. They allow automatic landslide modeling, mapping, detection, and assessment. LiDAR products, such as very

high-resolution DTM and slope angles, are widely utilized to define the geomorphological features of landslide, such as foot, mobilized materials, and scarps. ALS applications in landslides mapping are increasing with the development of these techniques, especially their horizontal and vertical accuracies. The main utilize of LiDAR point cloud is to produce a very high-resolution DTM. However, many factors can be obtained from terrain models, which considerably support landslide modeling and mapping. MLS and TLS techniques are commonly used to investigate the detailed characteristics of small-scale rockfall modeling. TLS is efficient for characterizing rock instabilities and for estimating volumes of mobilized materials. TLS is more effective than MLS and ALS for such applications because rock instabilities are controlled by locally planar structures. The high density of point clouds acquired through MLS and TLS also enable researchers to derive accurate discontinuity set orientations and slope profiles.

The rockfall risk assessment vary significantly relying on the landslide type, the techniques used for collecting input data, the considered exposed elements, and the scale of the analysis. Quantitative assessment produces more objective and comparable hazard and risk outcomes than the qualitative method. The cases demonstrated in this paper summarize the progress experienced in rockfall hazard and risk in last decade. The main challenge in quantitative rockfall hazard zoning at both regional and local scales is the hazard spatial distribution which are better described by the kinetic energy rather than by the size (magnitude) of the incident.

The progress produced in the analysis of the vulnerability of the exposed elements has benefited the risk assessment. The vulnerability derived can be directly combined in the risk assessment. Nevertheless, such methods need the consideration of a wide variation of structural arrays and typologies which analyses are not yet available.

In spite of this advancement, further studies are still needed before rockfall risk assessment could become a routine. Identifying the magnitude of the probable rockfall is still a challenge. Frequency–magnitude relationships are basic input data for quantitative hazard and risk assessment, though the lack of good quality historical and geological data in different areas restricts its implementation. On the other hand, frequency–magnitude evaluation assumes the presence of constant conditions for both slopes and triggers. However, this assumption is arguable in some geological contexts, especially in alpine mountainous areas. The fragmentation mechanism is not presently involved in trajectory modeling and may highly impact the reliability and validity of the outcomes. The rockfalls detachment without taking into account their fragmentation will lead to unrealistic runout distance and impact energy in excess of what should be expected. Conventional methods utilized

in risk assessment tend to simplify risk in two major parts: hazard and vulnerability. However, practical application of rockfall risk assessment has shown that exposure; especially for mobile features at risk (persons, trains, and cars) has a high impact in the probability of loss of life and on the risk results.

## Compliance with Ethical Standards

**Conflict of interest** Authors declare that there is no conflict of interest whatsoever.

## References

- Abellán A, Oppikofer T, Jaboyedoff M, Rosser NJ, Lim M, Lato MJ (2014) Terrestrial laser scanning of rock slope instabilities. *Earth Surf Process Landf* 39(1):80–97. <https://doi.org/10.1002/esp.3493>
- Agliardi F, Crosta G (2003) High resolution three-dimensional numerical modeling of rockfalls. *Int J Rock Mech Min Sci* 40(4):455–471. [https://doi.org/10.1016/S1365-1609\(03\)00021-2](https://doi.org/10.1016/S1365-1609(03)00021-2)
- Agliardi F, Crosta GB, Frattini P (2009) Integrating rockfall risk assessment and countermeasure design by 3D modelling techniques. *Nat Hazards Earth Syst Sci* 9:1059–1073
- Akgün A, Yakut M (2017) A rockfall hazard assessment for a residential area by using 2D and 3D simulation models: a case study from North Turkey. In: EGU general assembly conference abstracts, vol 19, p 2516
- Ardizzone F, Cardinali M, Galli M, Guzzetti F, Reichenbach P (2007) Identification and mapping of recent rainfall-induced landslides using elevation data collected by airborne LiDAR. *Nat Hazards Earth Syst Sci* 7(6):637–650. <https://hal.archives-ouvertes.fr/hal-00299461>
- Ashraf I, Hur S, Park Y (2017) An investigation of interpolation techniques to generate 2D intensity images from LiDAR data. *IEEE Access*. <https://doi.org/10.1109/ACCESS.2017.2699686>
- Azzoni A, La Barbera G, Zaninetti A (1995) Analysis and prediction of rockfalls using a mathematical model. *Int J Rock Mech Min Sci & Geomech Abstr* 32(7):709–724
- Bornaz L, Lingua ARF (2002) Engineering and environmental applications of laser scanner techniques. *Int Arch Photogramm Remote Sens Spat Inf Sci* 34(3/B):40–43
- Brabb E (1984) Innovative approaches for landslide hazard evaluation. IV International Symposium on Landslides, Toronto, pp 307–323
- Budetta P, Nappi M (2013) Comparison between qualitative rockfall risk rating systems for a road affected by high traffic intensity. *Nat Hazards Earth Syst Sci* 13(6):1643–1653. <https://doi.org/10.5194/nhess-13-1643-2013>
- Bui DT, Tuan TA, Klempe H, Pradhan B, Revhaug I (2016) Spatial prediction models for shallow landslide hazards: a comparative assessment of the efficacy of support vector machines, artificial neural networks, kernel logistic regression, and logistic model tree. *Landslides* 13(2):361–378. <https://doi.org/10.1007/s10346-015-0557-6>
- Bozzolo D, Pamini R, (1986) Simulation of rock falls down a valley side. *Acta Mechanica* 63(1–4):113–130
- Chen XL, Liu CG, Chang ZF, Zhou Q (2016) The relationship between the slope angle and the landslide size derived from limit equilibrium simulations. *Geomorphology* 253:547–550. <https://doi.org/10.1016/j.geomorph.2015.01.036>
- Chen Z, Gao B, Devereux B (2017) State-of-the-art: DTM generation using airborne LiDAR data. *Sensors* 17(1):150. <https://doi.org/10.3390/s17010150>
- Chow TE, Hodgson ME (2009) Effects of LiDAR post-spacing and DEM resolution to mean slope estimation. *Int J Geogr Inf Sci* 23(10):1277–1295. <https://doi.org/10.1080/13658810802344127>
- Christen M, Bartelt P, Gruber U (2007) RAMMS—a modeling system for snow avalanches, debris flows and rockfalls based on IDL. *Photogramm Fernerkund Geoinf* 4:289
- Corominas J, van Westen C, Frattini P, Cascini L, Malet JP, Fotopoulou S et al (2014) Recommendations for the quantitative analysis of landslide risk. *Bull Eng Geol Environ* 73(2):209–263
- Crosta GB, Agliardi F (2003) New methodology for physically-based rockfall hazard assessment. *Nat Hazards Earth Syst Sci* 3:407–422. <https://hal.archives-ouvertes.fr/hal-00301598>
- Crosta GB, Agliardi F, Frattini P, Imposimato S (2004) A three dimensional hybrid numerical model for rockfall simulation. *Geophys Res Abstr* 6:04502
- Crosta GB, Agliardi F, Frattini P, Lari S (2015) Key issues in rock fall modeling, hazard and risk assessment for rockfall protection. *Eng Geol Soc Territ* 2:43–58. [https://doi.org/10.1007/978-3-319-09057-3\\_4](https://doi.org/10.1007/978-3-319-09057-3_4)
- Cundall PA (1971) A computer model for simulating progressive, large-scale movements in blocky rock system. *Geotechnique* 29(1):47–65
- Daehne A, Corsini A (2013) Kinematics of active earthflows revealed by digital image correlation and DEM subtraction techniques applied to multi-temporal LiDAR data. *Earth Surf Process Landf* 38:640–654. <https://doi.org/10.1002/esp.3351>
- Dorren LKA (2016) A review of rockfall mechanics and modelling approaches. *Prog Phys Geogr* 27(1):69–87
- Dorren LKA (2012) Rockyfor3D (v5.1) revealed—transparent description of the complete 3D rockfall model
- Dorren LKA, Berger FPU (2006) Real-size experiments and 3-D simulation of rockfall on forested and non-forested slopes. *Nat Hazards Earth Syst Sci* 6:145–153. <https://doi.org/10.5194/nhess-6-145-2006>
- Dorren LKA, Seijmonsbergen AC (2003) Comparison of three GIS-based models for predicting rockfall runout zones at a regional scale. *Geomorphology* 56(1–2):49–64. [https://doi.org/10.1016/S0169-555X\(03\)00045-X](https://doi.org/10.1016/S0169-555X(03)00045-X)
- Dou J, Yamagishi H, Pourghasemi HR, Yunus AP, Song X, Xu Y et al (2015) An integrated artificial neural network model for the landslide susceptibility assessment of Osado Island, Japan. *Nat Hazards* 78(3):1749–1776. <https://doi.org/10.1007/s11069-015-1799-2>
- Evans JS, Hudak AT (2007) A multiscale curvature algorithm for classifying discrete return LiDAR in forested environments. *IEEE Trans Geosci Remote Sens* 45(4):1029–1038. <https://doi.org/10.1109/TGRS.2006.890412>
- Evans S, Hungr O (1993) The assessment of rockfall hazard at the base of talus slopes. *Can Geotech J* 30:620–636. <https://doi.org/10.1139/t93-054>
- Fanos AM, Pradhan B (2016) Multi-scenario rockfall hazard assessment using LiDAR data and GIS. *Geotech Geol Eng* 34(5):1375–1393. <https://doi.org/10.1007/s10706-016-0049-z>
- Fanos AM, Pradhan B, Aziz AA, Jebur MN, Park HJ (2016) Assessment of multi-scenario rockfall hazard based on mechanical parameters using high-resolution airborne laser scanning data and GIS in a tropical area. *Environ Earth Sci* 75(15):1129. <https://doi.org/10.1007/s12665-016-5936-3>
- Fernandes NF, Guimarães RF, Gomes RA, Vieira BC, Montgomery DR, Greenberg H (2004) Topographic controls of landslides in Rio de Janeiro: field evidence and modeling. *CATENA* 55(2):163–181. [https://doi.org/10.1016/S0341-8162\(03\)00115-2](https://doi.org/10.1016/S0341-8162(03)00115-2)

- Fityus S, Giacomini A, Buzzi O (2013) The significance of geology for the morphology of potentially unstable rocks. *Eng Geol* 162:43–52. <https://doi.org/10.1016/j.enggeo.2013.05.007>
- Fornaciai A, Bisson M, Landi P, Mazzarini F, Pareschi MT (2010) A LiDAR survey of Stromboli volcano (Italy): digital elevation model-based geomorphology and intensity analysis. *Int J Remote Sens* 31(12):3177–3194. <https://doi.org/10.1080/11431160903154416>
- Fratini P, Crosta G, Carrara A, Agliardi F (2008) Assessment of rockfall susceptibility by integrating statistical and physically-based approaches. *Geomorphology* 94(3–4):419–437. <https://doi.org/10.1016/j.geomorph.2006.10.037>
- Guzzetti F, Crosta G, Detti R, Agliardi F (2002) STONE: a computer program for the three dimensional simulation of rock-falls. *Comput Geosci* 28:1079–1093. [https://doi.org/10.1016/S0098-3004\(02\)00025-0](https://doi.org/10.1016/S0098-3004(02)00025-0)
- Habib AF, Kersting AP, Shaker A, Yan WY (2011) Geometric calibration and radiometric correction of LiDAR data and their impact on the quality of derived products. *Sensors* 11(9):9069–9097. <https://doi.org/10.3390/s110909069>
- Hungri O, Evans S (1988) Engineering evaluation of fragmental rockfall hazards. In: Proceedings of the fifth international symposium on landslides, Lausanne. AA Balkema, Rotterdam, pp 685–690
- Jaboyedoff M, Labiouse V (2011) Technical note: preliminary estimation of rockfall runout zones. *Nat Hazards Earth Syst Sci* 11(3):819–828. <https://doi.org/10.5194/nhess-11-819-2011>
- Jaboyedoff M, Oppikofer T, Abellán A, Derron MH, Loye A, Metzger R et al (2012) Use of LiDAR in landslide investigations: a review. *Nat Hazards* 61:5–28. <https://doi.org/10.1007/s11069-010-9634-2>
- Jahromi AB, Zoj MJV, Mohammadzadeh A, Sadeghian S (2011) A novel filtering algorithm for bare-earth extraction from airborne laser scanning data using an artificial neural network. *IEEE J Sel Top Appl Earth Obs Remote Sens* 4(4):836–843. <https://doi.org/10.1109/JSTARS.2011.2132793>
- Katz O, Morgan JK, Aharonov E, Dugan B (2014) Controls on the size and geometry of landslides: insights from discrete element numerical simulations. *Geomorphology* 220:104–113. <https://doi.org/10.1016/j.geomorph.2014.05.021>
- Kavzoglu T, Sahin EK, Colkesen I (2014) Landslide susceptibility mapping using GIS-based multi-criteria decision analysis, support vector machines, and logistic regression. *Landslides* 11(3):425–439. <https://doi.org/10.1007/s10346-013-0391-7>
- Kraus K, Pfeifer N (1998) Determination of terrain models in wooded areas with airborne laser scanner data. *ISPRS J Photogramm Remote Sens* 53(4):193–203. [https://doi.org/10.1016/S0924-2716\(98\)00009-4](https://doi.org/10.1016/S0924-2716(98)00009-4)
- Kritikos T, Davies T (2015) Assessment of rainfall-generated shallow landslide/debris-flow susceptibility and runout using a GIS-based approach: application to western Southern Alps of New Zealand. *Landslides* 12(6):1051–1075. <https://doi.org/10.1007/s10346-014-0533-6>
- Lambert S, Bourrier F (2013) Design of rockfall protection embankments: A review. *Eng Geol* 154:77–88
- Lambert S, Bourrier F, Toe D (2013) Improving three-dimensional rockfall trajectory simulation codes for assessing the efficiency of protective embankments. *Int J Rock Mech Min Sci* 60:26–36. <https://doi.org/10.1016/j.ijrmm.2012.12.029>
- Lan HX, Martin CD, Lim CH (2007) RockFall analyst: a GIS extension for three-dimensional and spatially distributed rockfall hazard modeling. *Comput Geosci* 33:262–279. <https://doi.org/10.1016/j.cageo.2006.05.013>
- Leine RI, Schweizer A, Christen M, Glover J, Bartelt P, Gerber W (2014) Simulation of rockfall trajectories with consideration of rock shape. *Multibody Syst Dyn* 32:241–271. <https://doi.org/10.1007/s11044-013-9393-4>
- Li L, Lan H (2015) Probabilistic modeling of rockfall trajectories: a review. *Bull Eng Geol Environ* 74(4):1163–1176. <https://doi.org/10.1007/s10064-015-0718-9>
- Messenzehl K, Meyer H, Otto JC, Hoffmann T, Dikau R (2016) Regional-scale controls on the spatial activity of rockfalls (Turtmann Valley, Swiss Alps)—a multivariate modeling approach. *Geomorphology* 287:29–45. <https://doi.org/10.1016/j.geomorph.2016.01.008>
- Mezaal MR, Pradhan B (2018) Data mining-aided automatic landslide detection using airborne laser scanning data in densely forested tropical areas. *Korean J Remote Sens* 34(1):45–74. <https://doi.org/10.7780/kjrs.2018.34.1.4>
- Mezaal MR, Pradhan B, Shafri HZM, Yusoff ZM (2017a) Automatic landslide detection using Dempster–Shafer theory from LiDAR-derived data and orthophotos. *Geomat Nat Hazards Risk* 8(2):1935–1954
- Mezaal MR, Pradhan B, Sameen MI, Mohd Shafri HZ, Yusoff ZM (2017b) Optimized neural architecture for automatic landslide detection from high-resolution airborne laser scanning data. *Appl Sci* 7(7):730. <https://doi.org/10.3390/app7070730>
- Nefeslioglu HA, Duman TY, Durmaz S (2008) Landslide susceptibility mapping for a part of tectonic Kelkit Valley (Eastern Black Sea region of Turkey). *Geomorphology* 94(3):401–418. <https://doi.org/10.1016/j.geomorph.2006.10.036>
- Pantelidis L (2011) A critical review of highway slope instability risk assessment systems. *Bull Eng Geol Environ* 70(3):395–400. <https://doi.org/10.1007/s10064-010-0328-5>
- Peng L, Niu R, Huang B, Wu X, Zhao Y, Ye R (2014) Landslide susceptibility mapping based on rough set theory and support vector machines: a case of the Three Gorges area, China. *Geomorphology* 204:287–301. <https://doi.org/10.1016/j.geomorph.2013.08.013>
- Petley DN (2013) Characterizing giant landslides. *Science* 339(6126):1395–1396. <https://doi.org/10.1126/science.1236165>
- Piteau DR, Clayton R (1976) Computer rockfall model. In: Proceedings of the meeting on rockfall dynamics and protective works effectiveness, Bergamo, Italy, ISMES Publication 90, pp 123–125
- Pradhan B, Fanos AM (2017a) Rockfall Hazard Assessment: An Overview. In: Pradhan B (ed) *Laser Scanning Applications in Landslide Assessment*. Springer, Cham, pp 299–322. [https://doi.org/10.1007/978-3-319-55342-9\\_15](https://doi.org/10.1007/978-3-319-55342-9_15)
- Pradhan B, Fanos AM (2017b) Application of LiDAR in rockfall hazard assessment in tropical region. In: Pradhan B (ed) *Laser scanning applications in landslide assessment*. Springer, Cham, pp 323–359. [https://doi.org/10.1007/978-3-319-55342-9\\_16](https://doi.org/10.1007/978-3-319-55342-9_16)
- Pradhan B, Sameen MI (2017) Laser scanning systems in landslide studies. In: Pradhan B (ed) *Laser scanning applications in landslide assessment*. Springer, Cham, pp 3–19. [https://doi.org/10.1007/978-3-319-55342-9\\_1](https://doi.org/10.1007/978-3-319-55342-9_1)
- Pradhan B, Yusof NM (2017) Slope vulnerability and risk assessment using high-resolution airborne laser scanning data. In: Pradhan B (ed) *Laser scanning applications in landslide assessment*. Springer, Cham, pp 235–251. [https://doi.org/10.1007/978-3-319-55342-9\\_12](https://doi.org/10.1007/978-3-319-55342-9_12)
- Pradhan B, Jebur MN, Abdullahi S (2017) Spatial prediction of landslides along jalan kota in bandar seri begawan (Brunei) using airborne LiDAR data and support vector machine. In: Pradhan B (ed) *Laser scanning applications in landslide assessment*. Springer, Cham, pp 167–178. [https://doi.org/10.1007/978-3-319-55342-9\\_9](https://doi.org/10.1007/978-3-319-55342-9_9)
- Rammer W, Brauner M, Dorren LKA, Berger F, Lexer MJ (2010) Evaluation of a 3-D rockfall module within a forest patch model. *Nat Hazards Earth Syst Sci* 10:699–711. <https://hal.archives-ouvertes.fr/hal-00585011>
- Regmi AD, Devkota KC, Yoshida K, Pradhan B, Pourghasemi HR, Kumamoto T, Akgun A (2014) Application of frequency ratio,

- statistical index, and weights-of-evidence models and their comparison in landslide susceptibility mapping in Central Nepal Himalaya. *Arab J Geosci* 7(2):725–742. <https://doi.org/10.1007/s12517-012-0807-z>
- Ritchie AM (1963) Evaluation of rockfall and its control. *Highw Res Rec* 17:13–28
- RocPro3D (2014) RocPro3D software
- Rocscience Inc (2013) RocFall 5.0
- Roering JJ, Mackey BH, Marshall JA, Sweeney KE, Deligne NI, Booth AM et al (2013) Connecting the dots with airborne LiDAR for geomorphic fieldwork. *Geomorphology* 200:172–183. <https://doi.org/10.1016/j.geomorph.2013.04.009>
- Rosser NJ, Brain MJ, Petley DN, Lim M, Norman EC (2013) Coastline retreat via progressive failure of rocky coastal cliffs. *Geology* 41(8):939–942. <https://doi.org/10.1130/G34371.1>
- Scaioni M, Longoni L, Melillo V, Papini M (2014) Remote sensing for landslide investigations: an overview of recent achievements and perspectives. *Remote Sens* 6(10):9600–9652
- Scioldo G (1991) Rotomap: analisi statistica del rotolamento dei massi. Guida Informatica Ambientale, Patron, Milano, pp 81–84 (in Italian)
- Sithole G, Vosselman G (2001) Filtering of laser altimetry data using a slope adaptive filter. *Int Arch Photogramm Remote Sens Spat Inf Sci* 34(3/W4):203–210
- Slatton KC, Carter WE, Shrestha RL, Dietrich W (2017) Airborne laser swath mapping: achieving the resolution and accuracy required for geosurficial research. *Geophys Res Lett* 34:23. <https://doi.org/10.1029/2007GL031939>
- Spadari M, Kardani M, De Carteret R, Giacomini A, Buzzi O, Fityus S, Sloan SW (2013) Statistical evaluation of rockfall energy ranges for different geological settings of New South Wales, Australia. *Eng Geol* 158:57–65. <https://doi.org/10.1016/j.engge.2013.03.007>
- van Dijke JJ, van Westen CJ (1990) Rockfall hazard: a geomorphologic application of neighbourhood analysis with ILWIS. *ITC J* 1:40–44
- Van Westen CJ, Rengers N, Terlien MTJ, Soeters R (1997) Prediction of the occurrence of slope instability phenomenal through GIS-based hazard zonation. *Geol Rundsch* 86:404–414. <https://doi.org/10.1007/s005310050149>
- Varnes D (1978) Slope movement types and processes. In: Schuster RL, Krizek RJ (eds) *Landslides: analysis and control*. Special Report No. 176. Transportation Research Board, National Academy of Science, Washington
- Volkwein A, Schellenberg K, Labiouse V, Agliardi F, Berger F, Bourrier F, Dorren LKA, Gerber W, Jaboyedo M (2011) Rockfall characterisation and structural protection—a review. *Nat Hazards Earth Syst Sci* 11(9):2617–2651. <https://hal.archives-ouvertes.fr/hal-00653458>
- Vosselman G (2000) Slope based filtering of laser altimetry data. *Int Arch Photogramm Remote Sens* 33(B3/2; PART 3):935–942
- Wang G, Joyce J, Phillips D, Shrestha R, Carter W (2013) Delineating and de-fining the boundaries of an active landslide in the rainforest of Puerto Rico using a combination of airborne and terrestrial LiDAR data. *Landslides* 10(4):503–513. <https://doi.org/10.1007/s10346-013-0400-x>
- Wendeler C, Leonhardt V, Luis R (2017) Flexible barriers composed of high-strength steel nets, as a solution to the near surface slides. In: *Workshop on world landslide forum*. Springer, Cham, pp 513–522. [https://doi.org/10.1007/978-3-319-53487-9\\_60](https://doi.org/10.1007/978-3-319-53487-9_60)
- Woltjer M, Rammer W, Brauner M, Seidl R, Mohren GMJ, Lexer MJ (2008) Coupling a 3D patch model and a rockfall module to assess rockfall protection in mountain forests. *J Environ Manag* 87:373–388. <https://doi.org/10.1016/j.jenvman.2007.01.031>
- Wu SS (1985) Rockfall evaluation by computer simulation. Publisher: Transportation Research Board, ISSN: 0361-1981
- Wyllie DC (2014) Calibration of rock fall modeling parameters. *Int J Rock Mech Min Sci* 67:170–180. <https://doi.org/10.1016/j.ijrmm.2013.10.002>
- Yan WY, Shaker A, Habib A, Kersting AP (2012) Improving classification accuracy of airborne LiDAR intensity data by geometric calibration and radiometric correction. *ISPRS J Photogramm Remote Sens* 67:35–44. <https://doi.org/10.1016/j.isprsjprs.2011.10.005>
- Yan WY, Shaker A, El-Ashmawy N (2015) Urban land cover classification using airborne LiDAR data: a review. *Remote Sens Environ* 158:295–310. <https://doi.org/10.1016/j.rse.2014.11.001>
- Zeng D, Wu L, Chen B, Shen W (2017) Slope-restricted multi-scale feature matching for geostationary satellite remote sensing images. *Remote Sens* 9(6):576. <https://doi.org/10.3390/rs9060576>
- Zhan Z, Lai B (2015) A novel DSM filtering algorithm for landslide monitoring based on multiconstraints. *IEEE J Sel Top Appl Earth Obs Remote Sens* 8(1):324–331. <https://doi.org/10.1109/JSTAR.2014.2319855>
- Zhang K, Chen SC, Whitman D, Shyu ML, Yan J, Zhang C (2003) A progressive morphological filter for removing nonground measurements from airborne LiDAR data. *IEEE Trans Geosci Remote Sens* 41(4):872–882. <https://doi.org/10.1109/TGRS.2003.810682>
- Zhang Y, Xiong X, Hu X (2013) Rigorous LiDAR strip adjustment with tri-angulated aerial imagery. *ISPRS Ann Photogramm Remote Sens Spat Inf Sci* 5(w2):361–366. <https://doi.org/10.5194/isprsnannals-II-5-W2-361-2013>
- Zhang Y, Xiong X, Zheng M, Huang X (2015) LiDAR strip adjustment using multifeatures matched with aerial images. *IEEE Trans Geosci Remote Sens* 53(2):976–987. <https://doi.org/10.1109/TGRS.2014.2331234>



**Biswajeet Pradhan** is the Senior Member of IEEE. He received the B.Sc. degree with honors from Berhampur University, India, the M.Sc. degree from the Indian Institute of Technology (IIT), Bombay, the M.Tech. degree in civil Engineering from the IIT, Kanpur, India, and Dresden University of Technology, Germany. He received the Ph.D. degree in GIS and geomatics engineering from the University Putra Malaysia. From 2008 to 2010, he was a recipient of Alexander von Humboldt Research

Fellowship from Germany. In 2011, he received his habilitation in “Remote Sensing” from Dresden University of Technology, Germany. Since March 2015, he is serving as the Humboldt Ambassador Scientist for the Alexander Von Humboldt Foundation, Germany. Dr. Pradhan is the recipient of prestigious German Academic Exchange Research (DAAD) Fellowship Award. He is currently a Distinguished Professor at Faculty of Engineering and IT, University of Technology Sydney. He has more than 18 years of teaching, research, consultancy, and industrial experience. Out of his more than 450 articles, more than 325 have been published in science citation index (SCI/SCIE) technical journals. He has written two books in GIS data compression and disaster management and edited three volumes, and written 12 book chapters. He specializes in remote sensing, GIS application, and soft computing techniques. He is listed as the World’s most highly cited researcher by ISI Thomson Reuter’s Report in 2017 and 2016.